Ecosystem carbon balance in the Hawaiian Islands under different scenarios of future climate and land use change

Paul C. Selmants[1], Benjamin M. Sleeter[2], Jinxun Liu[1], Tamara S. Wilson[1],

Clay Trauernicht[3], Abby G. Frazier[4,5], Gregory P. Asner[6]

Affiliations:

[1]U.S. Geological Survey, Moffett Field, CA, USA

[2]U.S. Geological Survey, Seattle, WA, USA

[3]University of Hawai‘i at Mānoa, Honolulu, HI, USA

[4]East-West Center, Honolulu, HI, USA

[5]Clark University, Worcester, MA, USA

[6]Arizona State University, Tempe, AZ, USA

Email: pselmants@usgs.gov

Running title: Hawai‘i carbon balance

Keywords: land use, climate change, carbon balance, Hawai‘i, scenarios, disturbance, ecosystem model

Date: October 08, 2021

Abstract

The State of Hawaiʻi passed legislation to be carbon neutral by 2045, a goal that will partly depend on carbon sequestration by terrestrial ecosystems. However, there is considerable uncertainty surrounding the future direction and magnitude of the land carbon sink in the Hawaiian Islands. We used the Land Use and Carbon Scenario Simulator (LUCAS), a spatially explicit stochastic simulation model that integrates landscape change and carbon gain-loss, to assess how projected future changes in climate and land use will influence ecosystem carbon balance in the Hawaiian Islands under all combinations of two radiative forcing scenarios (RCPs 4.5 and 8.5) and two land use scenarios (low and high) over a 90-year timespan from 2010-2100. Collectively, terrestrial ecosystems of the Hawaiian Islands acted as a net carbon sink under low radiative forcing (RCP 4.5) for the entire 90-year simulation period, with low land use change further enhancing carbon sink strength. In contrast, Hawaiian terrestrial ecosystems transitioned from a net sink to a net source of CO_2 to the atmosphere under high radiative forcing (RCP 8.5), with high land use accelerating this transition and exacerbating net carbon loss. A sensitivity test of the CO_2 fertilization effect on plant productivity revealed it to be a major source of uncertainty in projections of ecosystem carbon balance, highlighting the need for greater mechanistic understanding of plant productivity responses to rising atmospheric CO_2. Long-term model projections such as ours that incorporate the interactive effects of land use and climate change on regional ecosystem carbon balance will be critical to evaluating the potential of ecosystem-based climate mitigation strategies.

1. Introduction

Terrestrial ecosystems are a major sink for atmospheric carbon dioxide (CO_2), removing ~30% of human emissions on an annual basis and reducing the rate of increase in atmospheric CO_2 (Keenan and Williams 2018, Friedlingstein *et al* 2019). There is increasing recognition among policymakers that natural and agricultural ecosystems can contribute to climate mitigation, which has given rise to the popularity of "natural climate solutions" (Cameron *et al* 2017). Defined as conservation and land management efforts aimed at enhancing ecosystem carbon storage (Griscom *et al* 2017), natural climate solutions are appealing because they are seen as cost-efficient and readily available (Galarraga *et al* 2017, Cameron *et al* 2017, Fargione *et al* 2018). However, effective implementation is complicated by the uncertainty surrounding the future direction and magnitude of the land carbon sink, especially at the regional scale. Despite this uncertainty, evidence indicates that both interannual and long-term variability in carbon uptake by land ecosystems is driven primarily by fluctuations in climate, land use, and land cover change (Ahlström *et al* 2015, Prestele *et al* 2017, Friedlingstein *et al* 2019). Incorporating the interactive effects of land use and climate into spatially explicit future projections of ecosystem carbon balance could therefore provide a reference point to evaluate the effectiveness of land-based mitigation. Although a complex challenge, a growing number of sub-national jurisdictions plan to incorporate land-based mitigation strategies into their emissions reduction efforts. These jurisdictions would benefit from understanding how future land use and climate-biosphere feedbacks will affect ecosystem carbon balance in their respective regions (Sleeter *et al* 2019).

The State of Hawai‘i exemplifies the challenges associated with projecting the interactive effects of future climate and land use change on ecosystem carbon balance at a regional scale. Hawai‘i was the first U.S. state to enact legislation committing to full carbon neutrality, requiring the state to account for and offset all of its greenhouse gas emissions by 2045 (State of Hawai‘i Acts 15 and 16). This legislation emphasizes the mitigation potential of natural ecosystems as a key component to emissions reduction, necessitating baseline estimates and future projections of land carbon sink strength. However, Hawai‘i's challenging terrain complicates these assessment efforts. The main Hawaiian Islands are a complex mosaic of natural and human-dominated landscapes overlain by steep climate gradients across relatively short distances, with mean annual temperature ranging from ~4-24° C (Giambelluca *et al* 2014) and mean annual rainfall ranging from ~200-10,200 mm (Giambelluca *et al* 2013). Temperatures have risen rapidly in the

Hawaiian Islands since the mid 1970s (Giambelluca *et al* 2008, McKenzie *et al* 2019) and a long-term drying trend has persisted since the early 1920s (Frazier and Giambelluca 2017), resulting in reduced forest biomass and productivity (Barbosa and Asner 2017). These same drying and warming trends have increased the frequency and intensity of wildland fire (Trauernicht *et al* 2015, Trauernicht 2019) with predictable negative effects on ecosystem carbon balance (Selmants *et al* 2017). Ecosystem carbon stocks across the main Hawaiian Islands have also been strongly influenced by the legacy of past land use change (Osher *et al* 2003, Asner *et al* 2011). Thousands of hectares were deforested beginning in the late 19th century to clear land for sugar plantations and cattle pasture (Cuddihy and Stone 1990). Since the mid-20th century, much of this agricultural land has been steadily converted to urban areas, commercial forestry plantations, or simply abandoned and colonized by non-native grass and shrub species (Suryanata 2009, Perroy *et al* 2016). Although these past trends surely inform the future impact of climate and land use change on ecosystem carbon balance, high spatial and temporal heterogeneity complicates realistic projection efforts. To date only one study has attempted to integrate land use, climate, and natural disturbances into future projections of Hawaiian ecosystem carbon balance, with projections limited to the mid-21st century under a single land use change scenario and a single moderate radiative forcing scenario [Special Report on Emission Scenarios [SRES] A1B, equivalent to Representative Concentration pathway [RCP] 6; Selmants *et al* (2017)].

We used a stochastic, spatially explicit simulation model to estimate ecosystem carbon balance for Hawaiʻi's natural and agricultural lands on an annual basis for the period 2010–2100 under a range of assumptions about future climate, land use, land cover, disturbance, and global CO_2 emissions (Daniel *et al* 2016, 2018, Sleeter *et al* 2019). We developed four unique scenarios that explored different pathways, or future trajectories, of land use and climate change. These four scenarios represent all combinations of two land use change pathways (low and high) and two radiative forcing pathways (representative concentration pathway [RCP] 4.5 and RCP 8.5). In addition to these four scenarios, we conducted a separate series of simulations to examine how ecosystem carbon balance estimates vary in response to different levels of a CO_2 fertilization effect (CFE) on net primary productivity [NPP; Sleeter *et al* (2019)]. Our goals were to estimate statewide changes in Hawaiian ecosystem carbon balance and their uncertainties under a range of plausible future scenarios, quantify the relative impact of major controlling processes such as land use change, disturbance, and climate change, and assess the sensitivity of modeled ecosystem carbon balance estimates to varying levels of a CFE on NPP.

2. Methods

We used the Land Use and Carbon Scenario Simulator (LUCAS), an integrated landscape change and carbon gain-loss model, to project changes in ecosystem carbon balance for the seven main Hawaiian Islands. The landscape change portion of LUCAS is a state-and-transition model, where 'state' is the pre-defined information specific to each simulation cell (e.g., land cover class, climate zone) and 'transition' is the change in state of each simulation cell over time (Daniel *et al* 2016). Landscape change occurs by applying a Monte Carlo approach to track the state and age of each simulation cell in response to a pre-determined set of transition pathways (Daniel *et al* 2016). Transition pathways define which state types can be converted to any other state type. The carbon gain-loss portion tracks carbon stocks within each simulation cell over time as continuous state variables, along with a pre-defined set of continuous flows specifying rates of change in stock levels over time (Daniel *et al* 2018, Sleeter *et al* 2019). We parameterized the Hawai'i LUCAS model to estimate annual changes in carbon stocks and fluxes in response to land use, land use change, wildland fire, and long-term climate variability for the time period 2010-2100.

2.1 Study area

The spatial extent of this study was the terrestrial portion of the seven main Hawaiian Islands (figure 1), a total land area of 16,554 km^2. We subdivided this landscape into a grid of 264,870 simulation cells, each of which was 250 x 250 m in size. Each simulation cell was assigned to one of 210 possible state types based on the unique combination of seven islands, three moisture zones (dry, mesic, and wet; supplemental figure 1), and ten discrete land cover classes (figure 1). We also tracked the age and time since transition for each simulation cell as continuous state variables (Daniel *et al* 2016).

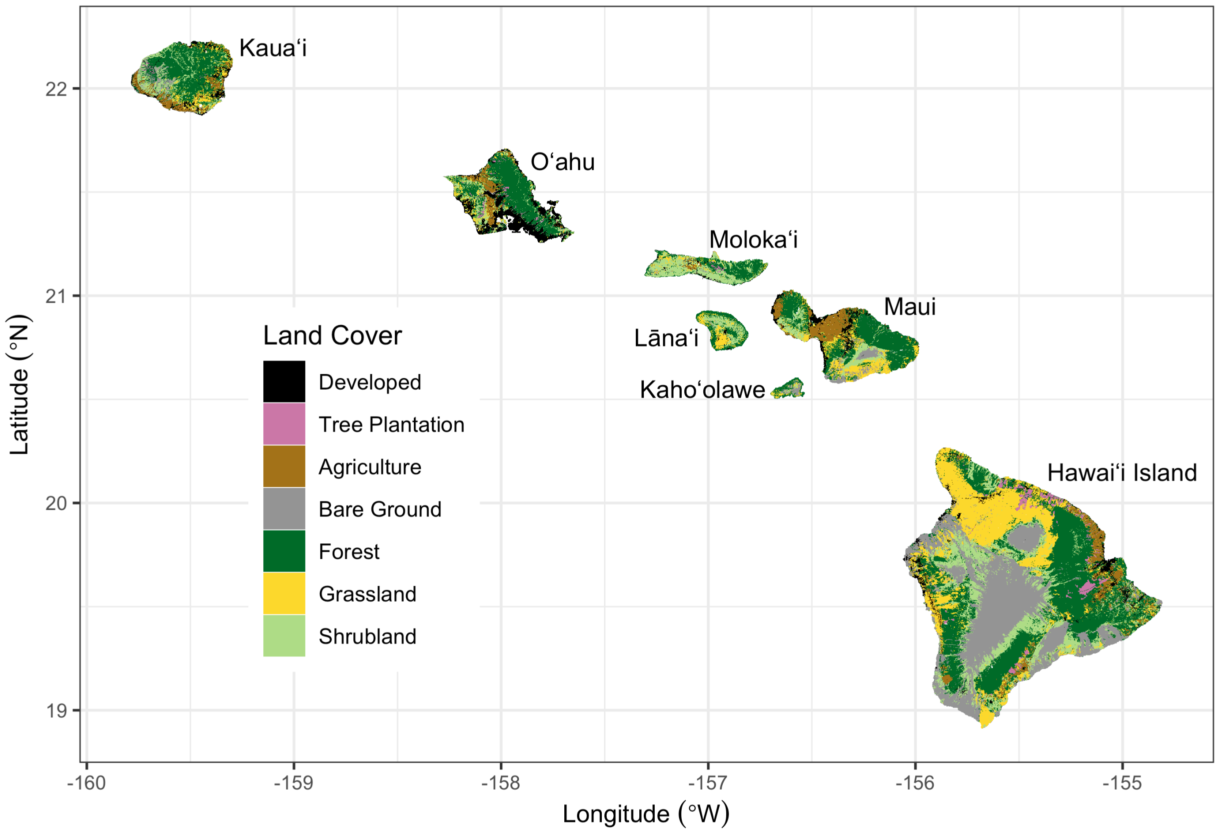

Figure 1: Land cover classification of the seven main Hawaiian Islands, adapted from Jacobi *et al.* (2017). Agriculture in this map combines herbaceous and woody crops, but these two crop types are treated as separate land cover classes in the simulation model. Water and Wetland land cover classes are not shown.

2.2 States and transitions

We developed two land use scenarios (low and high) with transition pathways modified from Daniel *et al* (2016). Transition pathways were pre-defined to represent urbanization, agricultural contraction, agricultural expansion, harvesting of tree plantations, and wildfire. Agriculture, forest, grassland, shrubland, and tree plantation land cover classes each had multiple transition pathways, i.e., they could each be converted into a variety of other land cover classes. The barren land cover class could only transition to developed, so its sole transition pathway was urbanization. Although most land cover classes had an urbanization transition pathway, there was no transition pathway out of an urbanized (developed) state. Water and wetland land cover classes remained static throughout the simulation period.

Transition targets set the area to be transitioned over time. These targets were based on either recent historical trends of land use change in the Hawaiian Islands from 1992-2011 (NOAA 2020) or on population projections for the State of Hawaiʻi (Kim and Bai 2018). For the high land use scenario, rates of agricultural contraction, agricultural expansion, and urbanization for each timestep and Monte Carlo realization were sampled from uniform distributions bounded by the median and maximum recent historical rates for each island. For the low land use scenario, rates of agricultural contraction and expansion were sampled from uniform distributions bounded by zero and the minimum recent historical rates for each island, which shifts the balance toward agricultural contraction and leads to a reduction in land area under active cultivation over time. Urbanization rates in the low land use scenario were based on island-level population estimates and projections at five year intervals from 2010-2045 (Kim and Bai 2018). We converted population projections into urbanization transition targets following Sleeter *et al* (2017) by calculating population density for each island and then projecting future developed area based on the five-year incremental change in island population. The spatial extent of agricultural contraction, agricultural expansion, and urbanization was constrained in both land use scenarios based on existing zoning maps (Daniel *et al* 2016). Transition targets for tree plantation harvest were set at ~75% of recent historical rates in the high land use scenario and ~40% of recent historical rates in the low land use scenario (Daniel *et al* 2016). Tree plantation forestry in the State of Hawaiʻi is primarily short-rotation (5-7 years) *Eucalyptus* spp., harvested at a rate of approximately 2 km^2 y^{-1} over the past decade. In both the high and low land use scenarios, approximately 60% of tree plantation harvests were replacement harvests resulting in conversion to grassland or agriculture. The remaining 40% were rotation harvests replanted to *Eucalyptus* spp. There was no transition pathway from any land cover class into tree plantation in either land use scenario, which is consistent with recent historical trends of stable or declining tree plantation land area since the year 2000. For the contemporary period (2010-2020), transition targets in both the high and low land use scenarios were set at low land use scenario rates and diverged after 2020.

The wildfire transition sub-model was modified from Daniel *et al* (2016) by incorporating a new 21-year historical wildfire spatial database of the Hawaiian Islands (supplemental figure 2). We used this new spatial database to calculate historical wildfire size distribution and ignition probabilities for each unique combination of moisture zone (supplemental figure 1), island, and land cover class (figure 1) for the years 1999-2019. Starting in 2020, the number and size of fires was randomly drawn from one of these historical year-sets for each timestep and Monte Carlo realization, using burn severity probabilities from Selmants *et al* (2017). Wildfire in the low land use scenario was sampled from the subset of historical fire years at or below the median area burned statewide from 1999-2019. The high land use scenario sampled from historical fire years above the median area burned over the same 21-year period (supplemental figure 2a). The vast majority of wildland fire in Hawai‘i is human-caused and initiates in non-native grasslands and shrublands (Trauernicht *et al* 2015), but can spread into nearby forest areas. Moderate to high severity fires that spread into mesic and wet forests can convert these areas into grasslands about half the time. However, moderate to high severity fires in mesic and wet forests account for < 5% of the total annual area burned, on average (Selmants *et al* 2017, Daniel *et al* 2018).

2.3 Carbon stocks and flows

The fate of carbon stocks was tracked for each simulation cell based on a suite of carbon flows (i.e., carbon fluxes) specifying the rates of change in these carbon stocks over time (Daniel *et al* 2018, Sleeter *et al* 2019). We defined carbon stocks as continuous state variables for each simulation cell, including live biomass, standing dead wood, down dead wood, litter, and soil organic carbon. We also included and tracked carbon in atmospheric, aquatic, and harvest product pools to enforce carbon mass balance (Daniel *et al* 2018). To transfer carbon between stocks, we defined baseline carbon flows as continuous variables resulting from growth, mortality, deadfall, woody decay, litter decomposition, and leaching (which includes runoff). We also defined carbon flows resulting from land use, land use change, and wildfire (Selmants *et al* 2017, Daniel *et al* 2018).

Initial carbon stocks and baseline carbon flows were derived from the Integrated Biosphere Simulator [IBIS; Foley *et al* (1996); Liu *et al* (2020)], a process-based dynamic global vegetation model. We initiated IBIS with minimal vegetation and simulated forward for 110 years using 30-year climate normals for the Hawaiian Islands [supplemental Figure 3; Giambelluca *et al* (2013); Giambelluca *et al* (2014)]. We calibrated IBIS carbon stocks with statewide gridded datasets of soil organic carbon (Soil Survey Staff 2016) and total forest live biomass. The total forest live biomass data was derived from Asner *et al* (2016) estimates of aboveground forest live biomass by applying a power function to calculate the belowground portion (Mokany *et al* 2006) as described in Selmants *et al* (2017). We calibrated gross photosynthesis in IBIS using a Hawai‘i-specific gridded dataset of gross primary production (GPP) derived from MODIS satellite imagery (Kimball *et al* 2017). Mean annual GPP from Kimball *et al* (2017) ranged from 0.123 - 3.88 kg C m^{-2} y^{-1} across the Hawaiian Islands, resulting in a NPP-to-GPP ratio ranging from 0.37 - 0.56.

We initiated net primary production in LUCAS for each simulation cell as the mean IBIS-derived value for each combination of moisture zone and land cover class (supplemental Table 1) adjusted with a set of spatially explicit stationary NPP multipliers to reflect local variation driven by microclimate [supplemental figure 5; Sleeter *et al* (2018); Sleeter *et al* (2019)]. The stationary spatial NPP multipliers were the NPP anomaly for each simulation cell relative to the mean empirically-derived NPP values for each state type (supplemental Figure 5). Soil carbon flux to the atmosphere (heterotrophic respiration, R_h) and aquatic soil carbon losses (leaching and overland flow) were estimated as the ratio of the IBIS-derived flux for each state type to the microclimate-adjusted NPP value for each simulation cell. We derived soil carbon loss as a fraction of NPP because photosynthesis is the dominant factor driving variation in ecosystem carbon fluxes, including R_h, and the vast majority of annual carbon loss from soils was fixed by photosynthesis within that year (Kuzyakov and Gavrichkova 2010, Baldocchi *et al* 2018). All other carbon flow rates were estimated as the ratio of the mean IBIS-derived flux for each state type to the size of the originating carbon stock at each age (Sleeter *et al* 2018, Daniel *et al* 2018). IBIS-derived carbon stocks for each state type were allowed to equilibrate with spatially variable NPP (supplemental figure 5) via a 100-year LUCAS spinup model run with no fire or land cover change and initiated with SSURGO soil carbon (Soil Survey Staff 2016) and IBIS values for live biomass, standing dead wood, down dead wood, and litter carbon stocks. Spatially variable carbon stocks from this spinup model run were used to initiate the main LUCAS model run.

Climate change impacts on carbon flows were represented by temporal growth and decay multipliers applied to each simulation cell based on mid-century (2049-2069) and end-of-century (2070-2099) statistically downscaled CMIP5 temperature and rainfall projections for the Hawaiian Islands under the RCP 4.5 and RCP 8.5 radiative forcing scenarios [supplemental figure 4; Elison Timm *et al* (2015); Elison Timm (2017)]. Annual increments in temporal growth and decay multipliers were calculated by dividing mid-century or end-of-century estimates by the number of intervening years. Temporal growth multipliers used to represent the impact of future changes in rainfall and temperature on NPP were calculated using empirical NPP equations (Schuur 2003, Del Grosso *et al* 2008) and climate model projections of temperature and rainfall for each radiative forcing scenario [supplemental figure 6; Sleeter *et al* (2019)]. Temporal decay multipliers used to represent the effect of future warming on turnover rates of dead organic matter were calculated using Q_{10} temperature coefficients based on climate model temperature projections for each radiative forcing scenario [supplemental figure 4; Elison Timm (2017)]. The Q_{10} temperature coefficients represented the proportional change in detrital carbon turnover due to a 10° C change in mean annual temperature. We applied a Q_{10} of 2.0 for wood and soil organic matter decay flows (Kurz *et al* 2009, Sleeter *et al* 2019) and a Q_{10} of 2.17 for litter decay flows

(Bothwell *et al* 2014). Transition-triggered carbon flows resulting from disturbances associated with land use change, timber harvesting, and wildfire were based on values from Don *et al* (2011), Selmants *et al* (2017), and Daniel *et al* (2018).

2.4 CO_2 fertilization effect

Increasing atmospheric CO_2 concentrations stimulate leaf-level photosynthesis, potentially increasing NPP as well (Franks *et al* 2013). However, the magnitude and persistence of this effect is highly uncertain, particularly across a range of climatic conditions and over long time spans (Walker *et al* 2020). Following Sleeter *et al* (2019), we developed a separate set of scenarios designed to test the sensitivity of LUCAS model projections of ecosystem carbon balance to different rates of a CO_2 fertilization effect (CFE). We incorporated a CFE multiplier for NPP that represented the percent increase in NPP for every 100 ppm increase in atmospheric CO_2 concentration under the high land use and high radiative forcing (RCP 8.5) scenario. We tested five CFE levels ranging from 5% to 15%, which is within the range of CFEs observed in free air CO_2 enrichment (FACE) experiments. For all CFE levels, we assumed a saturation point at an atmospheric CO_2 concentration of 600 ppm, with no further stimulation of NPP despite a continued increase in CO_2 concentration to 930 ppm by 2100. This 600 ppm threshold generally coincides with the upper limit from FACE experiments and is reached by the year 2060 under RCP 8.5.

2.5 Scenario simulations and analysis

Each of the four unique scenarios were run for 90 years at an annual timestep and repeated for 30 Monte Carlo realizations, using initial conditions corresponding to the year 2010. All simulations were performed within the SyncroSim (version 2.2.4) software framework with ST-Sim (version 3.2.13) and SF (version 3.2.10) add-on modules (Daniel *et al* 2016, 2018). Model input data and output summaries were prepared with the R statistical computing platform (R Core Team 2019) using the tidyverse (Wickham *et al* 2019), raster (Hijmans 2020), and rsyncrosim (Daniel *et al* 2020) packages. Carbon stocks and fluxes for the seven main Hawaiian Islands were calculated for each scenario by summing within each Monte Carlo realization on an annual basis and then calculating annual means as well as the annual upper and lower limits of the 30 Monte Carlo realizations. Carbon balance for the seven main Hawaiian Islands was calculated on annual basis for each scenario and Monte Carlo realization as net biome productivity (NBP), which was equal to annual carbon input in the form of NPP minus the annual sum of all carbon losses from terrestrial ecosystems, including heterotrophic respiration (R_h) from litter and soil, carbon fluxes to the atmosphere triggered by land use and land use change, wildfire emissions, and aquatic carbon losses through leaching and overland flow. Positive NBP values indicated ecosystems of the seven main Hawaiian Islands were acting as a net sink for atmospheric CO_2, while negative NBP values indicated that these ecosystems were acting as a net carbon source to the atmosphere (Chapin *et al* 2006).

3. Results

3.1 Carbon stocks and fluxes

Terrestrial ecosystems of the seven main Hawaiian Islands stored an estimated 316 Tg of carbon at the beginning of the simulation period in 2010 (figure 2a), with 58% in soil organic matter, 22% in living biomass, and 20% in surface dead organic matter (litter and dead wood; figure 2b). Ecosystems accumulated carbon in all scenarios but at different rates, with trajectories shaped primarily by climate change and to a lesser extent by land use change. The highest and most consistent projected accumulation of ecosystem carbon occured under the combination of low radiative forcing and low land use change, yielding a ~15% increase in ecosystem carbon to an average of 363 Tg by 2100 (figure 2a). In contrast, high radiative forcing and high land use change resulted in the lowest ecosystem carbon gain, reaching a peak of ~332 Tg in 2063 and a decline to 327 Tg in 2100, resulting in a net increase of only 3% by the end of the simulation period (figure 2a). Ecosystem carbon accumulation was driven exclusively by increasing soil organic carbon across all four scenarios, all other stocks declined over time (figure 2b).

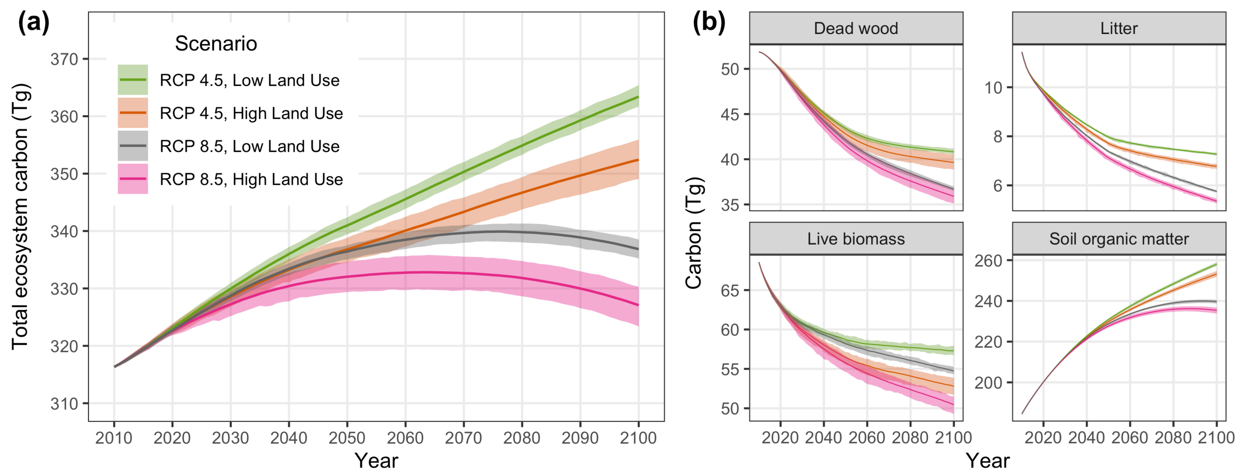

Figure 2: Projected changes in total ecosystem carbon storage (a) and individual carbon stocks (b) for the seven main Hawaiian Islands. Solid lines indicate the mean of 30 Monte Carlo realizations for each scenario, with shaded areas indicating the minimum and maximum range of Monte Carlo realizations.

Net primary production (NPP) for the seven main Hawaiian Islands was ~8.1 Tg y^{-1} at the beginning of the simulation period in 2010 (supplementary figure 5) with land use change driving an approximate 2% decline during the contemporary period (2010-2020). NPP continued to decline throughout the rest of the simulation period (2020-2100) across all four scenarios, but this long-term decline was driven primarily by climate change and to a lesser extent by land use change (Fig. 3). The combination of high radiative forcing (RCP 8.5) and high land use change led to the steepest decline in NPP over time, driven by intense long-term drying on the leeward sides of islands under RCP 8.5 (supplemental figures 4 and 6) and sustained losses of forest and shrubland land area in the high land use scenario (supplemental figure 7). In contrast, intense warming under RCP 8.5 (supplemental figure 4) led to an increase in heterotrophic respiration (R_h) in the latter half of the 21st century under the low land use scenario (figure 3), and R_h was 3% higher on average by 2100 in the RCP 8.5 radiative forcing scenario than in the RCP 4.5 radiative forcing scenario. Heterotrophic respiration declined substantially over time in the high land use scenario (figure 3) because of long-term reductions in forest and shrubland land area (supplemental figure 7), similar to trends in NPP. Transition-triggered carbon fluxes to the atmosphere from land use, land use change, and wildfire were largely independent of changes in climate, stabilizing by mid-century at an average of ~ 0.4 Tg y^{-1} in the high land use scenario and ~ 0.2 Tg y^{-1} in the low land use scenario (figure 3). Uncertainty around transition-triggered carbon fluxes were higher in the high land use scenario, driven primarily by greater variability in wildland fire probabilities.

3.2 Ecosystem carbon balance

Net biome productivity (NBP) averaged approximately 0.6 Tg C y^{-1} at the start of the simulation period and declined over time in all four scenarios (figure 4). On average, terrestrial ecosystems of the seven main Hawaiian Islands collectively acted as a net carbon sink under the RCP 4.5 radiative forcing scenario throughout the simulation period, but carbon sink strength was ~40% lower in the high land use scenario compared to the low land use scenario by the end of the simulation period (figure 4). In contrast, ecosystems of the Hawaiian Islands acted as a net carbon source to the atmosphere toward the latter half of the simulation period under RCP 8.5, with the transition from sink to source occuring 15 years earlier on average in the high land use scenario than in the low land use scenario (figure 4). The high land use scenario under RCP 8.5 represented a ~40% larger net source of carbon to the atmosphere by the year 2100 than the low-land use scenario under the same radiative forcing. Over the entire simulation period, both global emissions reductions and local avoided land conversion resulted in substantial increases in cumulative NBP (figure 5). However, switching from RCP 8.5 to RCP 4.5 increased cumulative NBP in the Hawaiian Islands more than twice as much as reducing emissions from local land use change and wildfire disturbance (figure 5). Switching from RCP 8.5 to RCP 4.5 under the low land use scenario yielded the greatest cumulative increase in NBP, resulting in a median gain of 26.5 Tg of carbon over the entire 90-year simulation period.

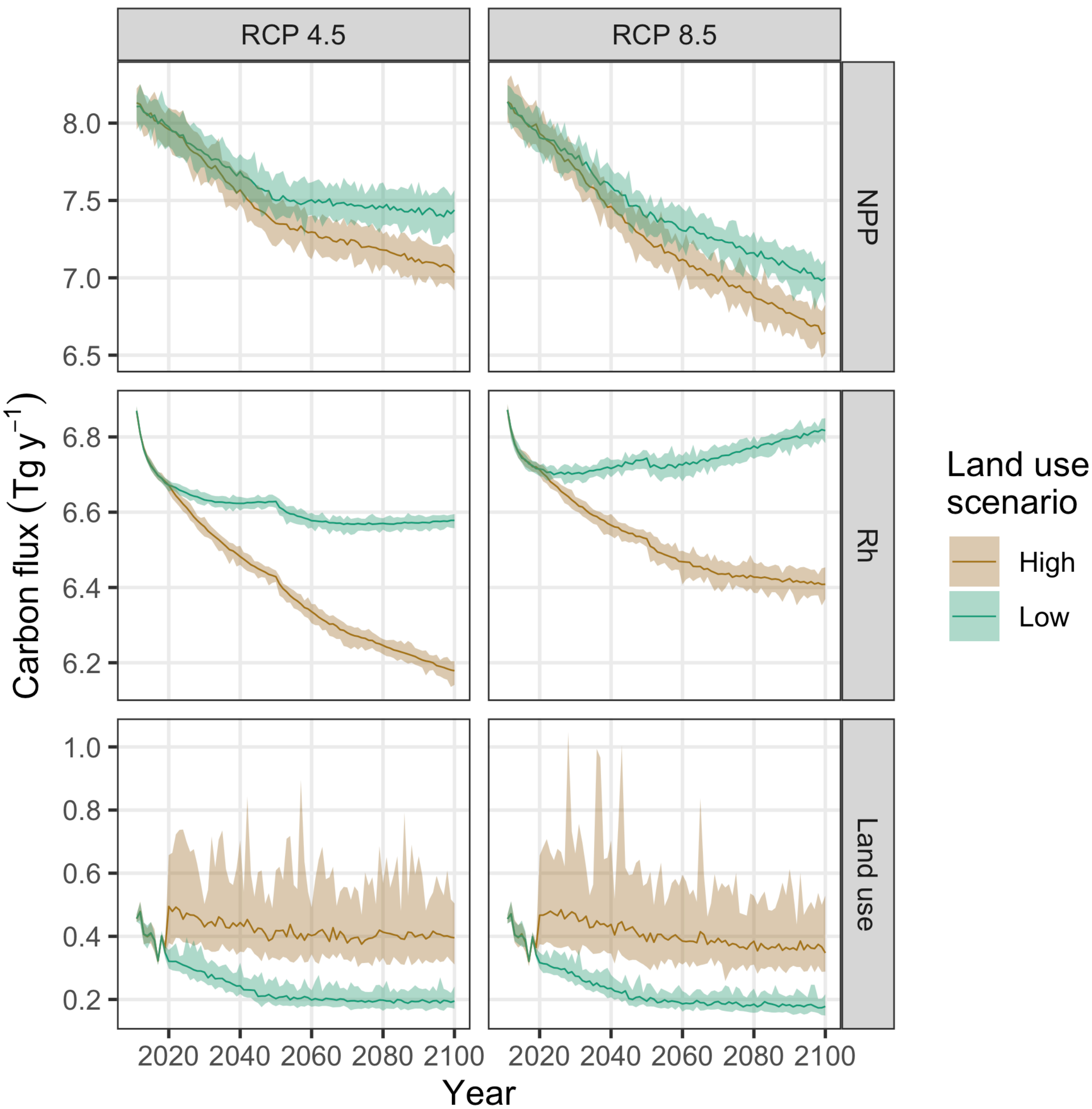

Figure 3: Projected changes in net primary production (NPP), heterotrophic respiration (Rh) and carbon fluxes induced by land use and land use change for the seven main Hawaiian Islands. Solid lines indicate the mean of 30 Monte Carlo realizations for each scenario, with shaded areas indicating the minimum and maximum range of Monte Carlo realizations.

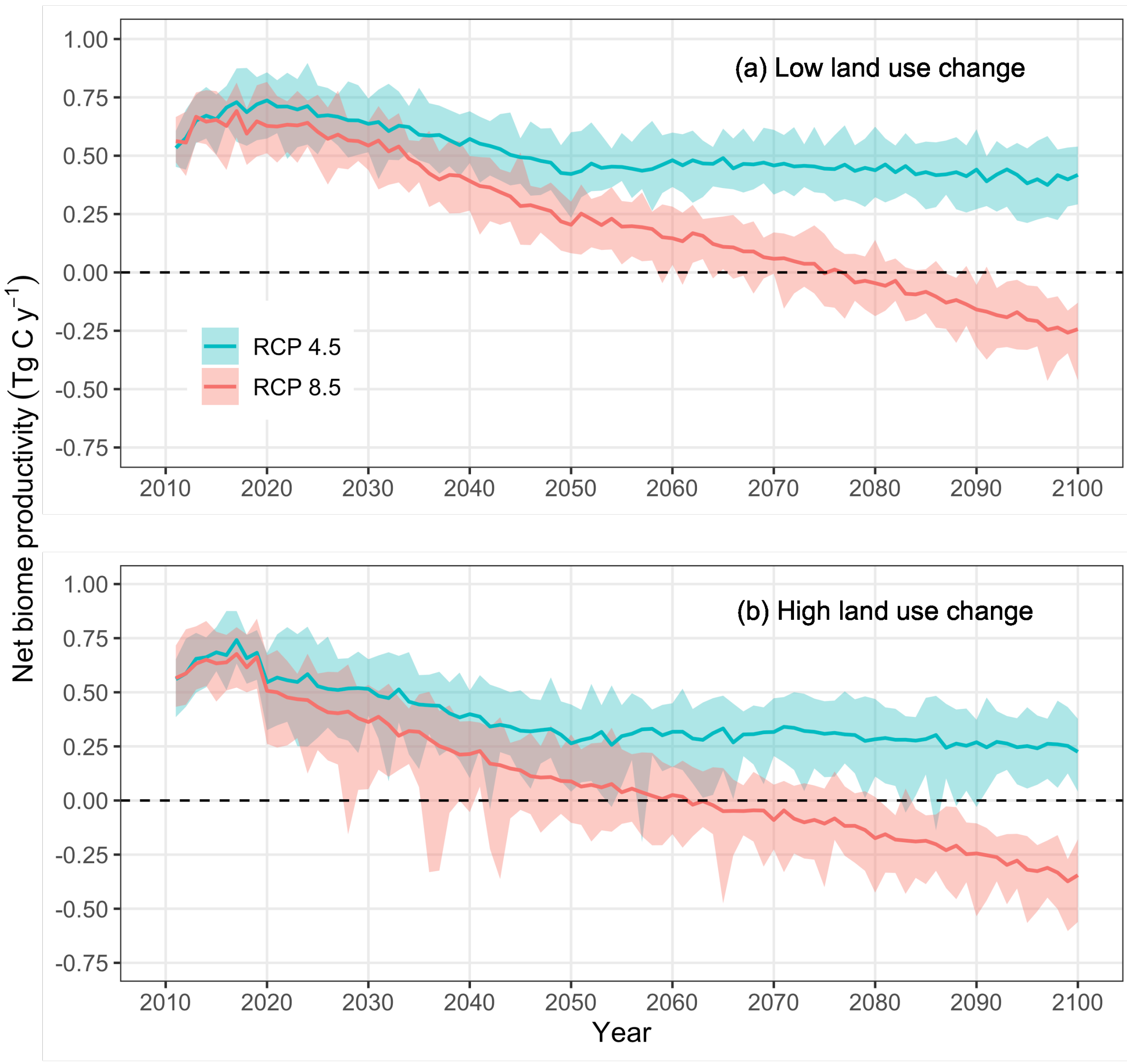

Figure 4: Projected changes in net biome productivity (NBP) for the seven main Hawaiian Islands. Solid lines indicate the mean of 30 Monte Carlo realizations for each scenario, with shaded areas indicating the minimum and maximum range of Monte Carlo realizations. The dashed horizontal line in each panel represents the boundary between ecosystems acting as a net carbon sink (positive NBP values) and a net carbon source (negative NBP values).

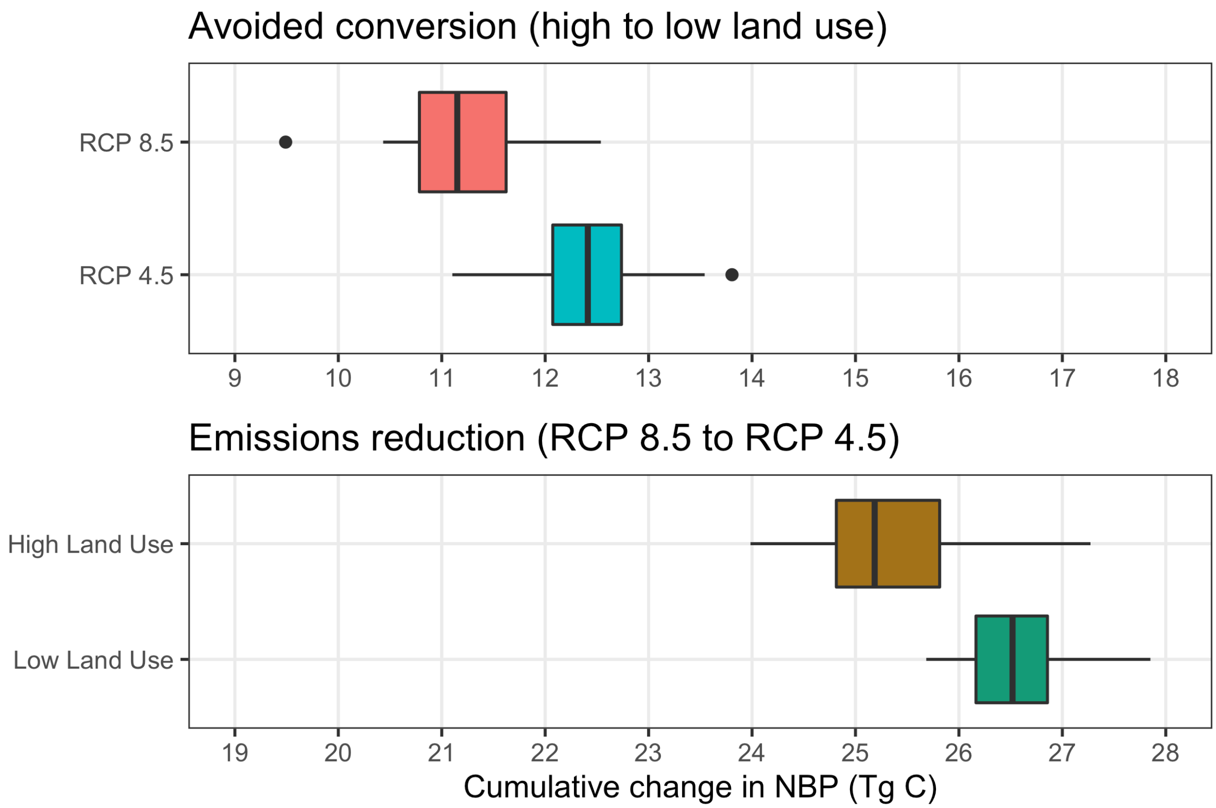

Figure 5: Projected changes in cumulative net biome productivity (NBP) for the seven main Hawaiian Islands when switching from the high to low land use change scenario under each radiative forcing scenario (top panel) and when switching from the high (RCP 8.5) to low (RCP 4.5) radiative forcing scenario under each land use scenario (bottom panel). Box plots indicate the median (vertical black line), 25th and 75th percentiles (colored boxes), 10th and 90th percentiles (thin horizontal lines), and values outside of this range (black circles). Note the different x-axis scales in each panel.

3.3 CO_2 fertilization effect

Projected estimates of both total ecosystem carbon storage and ecosystem carbon balance were highly sensitive to differing rates of a CFE on plant productivity. Under the high radiative forcing (RCP 8.5) and high land use scenario, the inclusion of a CFE ranging from 5-15% led to ~33-98 Tg of additional carbon storage in ecosystems by the end of the century, a ~10-30% increase (figure 6a). Compared to the reference scenario (0% CFE), a 5% CFE was sufficient to transform Hawaiian terrestrial ecosystems from a net carbon source to the atmosphere during the latter half of the 21st century (figure 4b) to a net carbon sink for the entire simulation period (figure 6b), completely offsetting all other carbon losses induced by high radiative forcing and high land use. Net carbon sink strength was further enhanced at higher CFE rates, with NBP increasing by an average of 0.07 Tg C y^{-1} for each 1% increase in CFE (figure 6b). When compared to other scenarios, applying a 5% CFE to the high radiative forcing and high land use scenario resulted in a mean annual NBP of 0.46 ± 0.3 Tg C y^{-1}, roughly equivalent to mean annual NBP in the low radiative forcing and low land use scenario with no CFE (0.52 ± 0.12). A 15% CFE applied to the high radiative forcing and high land use scenario resulted in a mean annual NBP of 1.18 ± 0.29 Tg C y^{-1}, more than double that of the low radiative forcing and low land use scenario with no CFE.

4. Discussion

We estimated that terrestrial ecosystems of the Hawaiian Islands have been a consistent net sink for atmospheric carbon over the last decade (figure 4). For the time period 2011-2019, net biome productivity (NBP) averaged 0.64 TgC y^{-1} and ranged from 0.46 to 0.88 TgC y^{-1} across all scenarios. Based on this mean annual NBP estimate, Hawaiian terrestrial ecosystems offset approximately 13% of 2015 statewide CO_2 emissions from energy production and transportation (5.04 Tg C), the State of Hawai‘i’s largest source of greenhouse gas emissions (State of Hawai‘i 2019). Future projections indicate Hawaiian terrestrial ecosystems will continue to be a net sink for atmospheric carbon if global CO_2 emissions peak around 2040 and then decline (RCP 4.5),

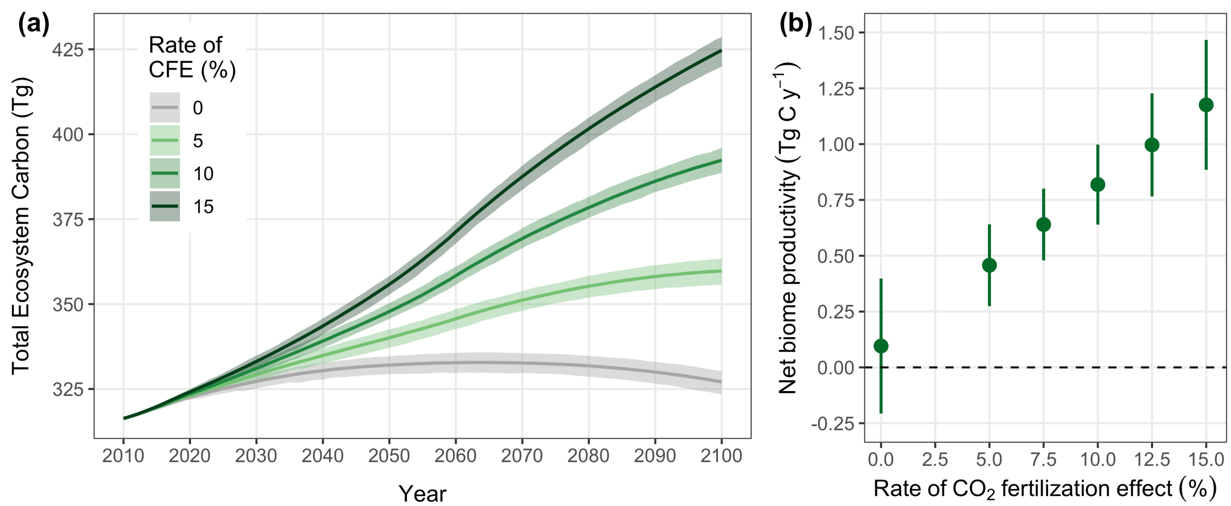

Figure 6: Sensitivity of projected changes in total ecosystem carbon storage (a) and mean annual net biome productivity (b) to different rates of a carbon dioxide fertilization effect (CFE) in the seven main Hawaiian Islands under the RCP 8.5 radiative forcing and high land use scenario. The CFE is the percent change in net primary productivity (NPP) for every 100 ppm increase in atmospheric carbon dioxide. Solid lines in (a) indicate mean total ecosystem carbon storage across 30 Monte Carlo realizations for each CFE rate, with shaded areas indicating the minimum and maximum range of Monte Carlo realizations. Solid circles in (b) represent mean annual net biome productivity averaged across all years and Monte Carlo realizations for each CFE rate, with vertical lines indicating the standard deviation of the mean. The dashed horizontal line in (b) represents the boundary between ecosystems acting as a net carbon sink (positive values) and a net carbon source (negative values).

and that carbon sink strength can be further enhanced by reducing the intensity and extent of future land use change. If, however, global CO_2 emissions continue to rise throughout the 21st century (RCP 8.5), our projections indicate Hawaiian ecosystems will transition from a net sink to a net source of CO_2 to the atmosphere, with high levels of land use change accelerating this transition and exacerbating net carbon loss. Our model results also indicate that projections of ecosystem carbon balance are highly sensitive to the introduction of a CFE. Even a 5% increase in NPP for every 100 ppm increase in atmospheric CO_2 was sufficient to completely offset all other carbon losses induced by the high radiative forcing and high land use scenario, maintaining Hawaiian Island ecosystems as a net carbon sink for the entire simulation period instead of transitioning to a net carbon source by mid-century. Reconciling the high uncertainty surrounding the response of net photosynthesis to rising atmospheric CO_2 is essential to more realistically constrain model projections of ecosystem carbon balance.

4.1 Impact of different climate and land use pathways

By comparing ecosystem carbon balance estimates under different scenario combinations, we were able to assess the relative impact of both global emissions reductions and regional actions to reduce emissions from land use, land use change, and wildland fire (figure 5). Global adherence to a lower emissions trajectory (i.e., switching from RCP 8.5 to RCP 4.5) had the largest impact, resulting in a median cumulative increase of 26 Tg C sequestered by Hawaiian ecosystems over the 90-year simulation period. Long-term reductions in the intensity of land use change also consistently led to an increase in ecosystem carbon sequestration, but to a lesser degree than global emissions reductions. Switching from the high to the low land use scenario resulted in a median cumulative retention of an additional 11.6 Tg C in Hawaiian ecosystems by 2100. The combination of global climate mitigation and local reductions in land use conversion had the largest potential benefit to ecosystem carbon sequestration, reducing cumulative net losses by over 400% (37.7 Tg C). Notably, the relative impact of reducing emissions from land use change was much greater under the high radiative forcing pathway (RCP 8.5). Cumulative NBP increased by 130% when switching from the high to low land use scenario under RCP 8.5, as opposed to a 37% cumulative increase in NBP when switching from high to low land use under RCP 4.5. These results demonstrate that reducing ecosystem carbon losses from land use change, harvest, and wildland fire can be an important component of greenhouse gas reduction efforts by sub-national jurisdictions like the State of Hawai‘i, regardless of the global emissions trajectory. These results also highlight the utility of Hawai‘i's multi-pronged approach of participating in global climate mitigation efforts by reducing emissions from the energy and transportation sectors while also reducing land use emissions to minimize positive feedbacks to the climate system.

4.2 Comparison to other studies

There are few estimates of contemporary ecosystem carbon balance for the main Hawaiian Islands, and even fewer model projections of future ecosystem carbon balance in response to climate and land use change. Our mean annual NBP estimate of 0.64 TgC y^{-1} for the period 2011-2020 agrees well with a recent State of Hawai‘i Greenhouse Gas Inventory report, which estimated an annual net carbon sink of 0.66 Tg C in 2015 from agriculture, forestry, and other land uses (State of Hawai‘i 2019). In contrast, our NBP estimate for the past decade was ~ 88% higher than a previous statewide LUCAS model estimate covering the same time period [0.341 Tg C y^{-1}; Selmants *et al* (2017)]. This discrepancy was likely driven by modifications in how we calculated NPP, soil R_h, and soil aquatic carbon loss compared to previous versions of the LUCAS model, as well our model's finer spatial resolution (Selmants *et al* 2017, Daniel *et al* 2018). Previous versions of a Hawai‘i LUCAS model were run at 1-km spatial resolution and simulation cells within each unique combination of moisture zone and state type all had the same mean IBIS-derived NPP value applied to them at the beginning of the simulation period. In contrast, our NPP estimates at 250-m spatial resolution were adjusted on a cell-by-cell basis using Hawai‘i-specific climate data [supplementary figure 3; Giambelluca *et al* (2013); Giambelluca *et al* (2014)] as described in section 2.3. As a result, our statewide NPP estimates from 2011-2020 were 9.5% lower on average than previous LUCAS model estimates for Hawai‘i during the same time period (Selmants *et al* 2017), likely because of the greater influence of more arid simulation cells. Soil carbon losses via R_h, leaching, and overland flow in previous versions of the LUCAS model were calculated as the ratio of the IBIS-derived flux to the size of the originating carbon stock, in this case soil organic carbon to 1-m depth (Daniel *et al* 2018). Here we calculated soil R_h and aquatic carbon losses as the ratio of the mean IBIS-derived flux to the microclimate-adjusted NPP value of each simulation cell, which is a more realistic driver than stock size (Kuzyakov and Gavrichkova 2010, Jackson *et al* 2017, Baldocchi *et al* 2018). Compared to previous Hawaiʻi LUCAS model estimates (Selmants *et al* 2017), soil R_h and aquatic carbon losses from 2011-2020 were reduced by an average of 15% and 21%, respectively, which widened the gap between between carbon gain (NPP) and carbon losses and accounted for the overall increase in NBP estimates for this time period.

4.3 Limitations of this study

There is ample evidence that increasing atmospheric CO_2 concentrations can stimulate NPP (Norby *et al* 2005, Zhu *et al* 2016), but the magnitude and persistence of this effect remains highly uncertain (Franks *et al* 2013, Walker *et al* 2020). Our results demonstrate that long-term projections of ecosystem carbon balance are highly sensitive to uncertainty in CFE strength. With no CFE, Hawaiian ecosystems became a net source of CO_2 to the atmosphere beginning in the latter half of the 21st century under the high land use and high radiative forcing scenario. However, a CFE equivalent to a 5% increase in NPP for every 100 ppm increase in atmospheric CO_2 applied to the same scenario resulted in Hawaiian ecosystems remaining a net carbon sink throughout the entire simulation period. A 15% CFE applied to the high land use and high radiative forcing scenario resulted in a nearly 5-fold increase in mean annual NBP averaged across all years and Monte Carlo realizations. Despite this demonstrated sensitivity to a CFE, several potentially attenuating factors complicate the selection of a realistic CFE value with any degree of confidence (Walker *et al* 2020). Nitrogen and phosphorus limitation can reduce or eliminate a CFE (Reich *et al* 2006, Norby *et al* 2010, He *et al* 2017, Terrer *et al* 2019), as can water limitation and heat stress (Obermeier *et al* 2017, Birami *et al* 2020). Forest age may also be a factor, with young aggrading forests showing a strong positive growth response to CO_2 fertilization (Walker *et al* 2019), while old-growth forests show little to no response (Jiang *et al* 2020, Yang *et al* 2020). This evidence indicates that a CFE may be highly variable across space and time, suggesting it may be unrealistic to apply a single CFE rate value across an entire region over several decades. Until mechanistic understanding is improved, the most conservative approach when projecting future ecosystem balance in the context of climate mitigation planning may be to assume no CFE, with the knowledge that any realized CFE will only enhance ecosystem carbon sequestration.

Our model does not currently differentiate between forests dominated by native versus non-native tree species, which could influence estimates of ecosystem carbon balance. Native forests in the Hawaiian Islands are dominated by ‘ōhi‘a (*Metrosideros polymorpha* Gauditch), an endemic foundational tree species found across a broad range of climatic and edaphic conditions (Ziegler 2002). Beginning in 2010, a fungal disease termed Rapid ‘Ōhi‘a Death (ROD) caused by two *Ceratocystus* spp. has emerged and caused widespread mortality to mature ‘ōhi‘a trees across a range of size classes, primarily on Hawai‘i Island (Mortenson *et al* 2016, Fortini *et al* 2019). The distribution and potential range of this emerging threat to Hawai‘i’s dominant native tree species have only recently been mapped (Vaughn *et al* 2018, Fortini *et al* 2019), but the pulse of newly dead organic matter and reduction in photosynthetic capacity induced by widespread tree mortality could significantly alter ecosystem carbon balance over the long-term (Sleeter *et al* 2019). ROD-affected forests could also undergo a replacement of canopy dominant stress-tolerating ‘ōhi‘a trees by non-native tree species with faster relative growth rates, lower wood density, and faster tissue turnover, potentially altering the long-term trajectory of carbon cycling in Hawaiian forest ecosystems. New model projections for Hawai‘i that incorporate ROD spread rates and forest restoration scenarios will therefore require differentiation among forest ecosystems dominated by native and non-native tree species.

Interannual climate variability is a primary factor influencing spatial and temporal patterns of global wildland fire activity (Abatzoglou *et al* 2018), with climate warming expected to increase wildland fire frequency and wildfire season length across a wide range of biomes (Sun *et al* 2019). Although our model projections capture the spatial and temporal variation in ignition probability and fire extent by sampling from previous fire years (1999-2019), we did not incorporate the effects of projected future climate change on the frequency and extent of wildland fire. Recent fire probability modeling for the northwest portion of Hawaiʻi Island indicated that projected drying and warming trends under RCP 8.5 could increase maximum fire probability values more than three-fold and shift areas of peak flammability to higher elevation by mid-century (Trauernicht 2019). Extending this probability fire modeling approach statewide would provide a quantitative, spatially explicit assessment of wildland fire probability for the main Hawaiian Islands as predicted by climate, land cover, and ignition density, which is highly correlated with population density (Trauernicht *et al* 2015, Trauernicht 2019). This approach would provide future simulation model projections of Hawaiian ecosystem carbon balance with more realistic scenarios of expected annual area burned based on the integrated effects of future climate and land use change.

5. Conclusion

Although terrestrial ecosystems are currently an important sink for atmospheric CO_2, the future direction and magnitude of the land carbon sink are highly uncertain, especially at regional scales. Our simulation modeling results indicated that projected climate change, dictated by long-term trajectories in global greenhouse gas emissions, was the primary factor influencing terrestrial ecosystem carbon balance in the Hawaiian Islands. Long-term reductions in the intensity of land use change and wildland fire also consistently led to an increase in ecosystem carbon sequestration, but to a lesser degree than global emissions reductions. CO_2 fertilization of NPP was the largest source of uncertainty in long-term projections of ecosystem carbon balance in the Hawaiian Islands, highlighting the need for greater mechanistic understanding of the cascading effects of rising atmospheric CO_2 on ecosystem carbon sequestration. By incorporating the interactive effects of land use and climate change into future projections of ecosystem carbon balance, our model results could be used as a set of baseline projections for the State of Hawai‘i to evaluate different ecosystem-based climate mitigation strategies. Studies like ours that incorporate stochasticity into spatially explicit simulation models could also provide a framework for the growing number of sub-national jurisdictions that plan to incorporate ecosystem carbon sequestration into their emissions reduction efforts. These long-term projections will be critical to assessing the impact of future land use change and climate-biosphere feedbacks on meeting climate mitigation goals.

Acknowledgements

This study was funded by the U.S. Geological Survey Biological Carbon Sequestration Program and the Pacific Islands Climate Adaptation Science Center. Thanks to Leonardo Frid and Colin Daniel of ApexRMS for assistance with SyncroSim software, and to Nicholas Koch of Forest Solutions, Inc. for information on *Eucalyptus* spp. harvesting in Hawai‘i. Thanks also to Christian Giardina and Zhiliang Zhu for providing the impetus for this research. Any use of trade, firm, or product names is for descriptive purposes only and does not imply endorsement by the U.S. Government.

Data and code availability

The data that support the findings of this study are openly available. LUCAS model tabular output data and metadata are available in machine readable format from the USGS ScienceBase repository at https://doi.org/10.5066/P9AWLFKZ. LUCAS model input data and R scripts used to format input data, summarize output data and compile this manuscript are available from a GitHub repository (https://github.com/selmants/HI_Model) archived at https://doi.org/10.5281/zenodo.5198072.

ORCID

Paul C. Selmants https://orcid.org/0000-0001-6211-3957

Benjamin M. Sleeter https://orcid.org/0000-0003-2371-9571

Jinxun Liu https://orcid.org/0000-0003-0561-8988

Tamara S. Wilson https://orcid.org/0000-0001-7399-7532

Clay Trauernicht https://orcid.org/0000-0002-1509-8536

Abby G. Frazier https://orcid.org/0000-0003-4076-4577

Gregory P. Asner https://orcid.org/0000-0001-7893-6421

References

Abatzoglou J T, Williams A P, Boschetti L, Zubkova M and Kolden C A 2018 Global patterns of interannual climate–fire relationships *Global Change Biology* **24** 5164–75 Online: https://onlinelibrary.wiley.com/doi/abs/10.1111/gcb.14405

Ahlström A, Raupach M R, Schurgers G, Smith B, Arneth A, Jung M, Reichstein M, Canadell J G, Friedlingstein P, Jain A K, Kato E, Poulter B, Sitch S, Stocker B D, Viovy N, Wang Y P, Wiltshire A, Zaehle S and Zeng N 2015 The dominant role of semi-arid ecosystems in the trend and variability of the land CO2 sink *Science* **348** 895–9 Online: https://science.sciencemag.org/content/348/6237/895

Asner G P, Hughes R F, Mascaro J, Uowolo A L, Knapp D E, Jacobson J, Kennedy-Bowdoin T and Clark J K 2011 High-resolution carbon mapping on the million-hectare Island of Hawaii *Frontiers in Ecology and the Environment* **9** 434–9 Online: http://doi.wiley.com/10.1890/100179

Asner G P, Sousan S, Knapp D E, Selmants P C, Martin R E, Hughes R F and Giardina C P 2016 Rapid forest carbon assessments of oceanic islands: A case study of the Hawaiian archipelago

Carbon Balance and Management **11** Online: http://www.cbmjournal.com/content/11/1/1

Baldocchi D, Chu H and Reichstein M 2018 Inter-annual variability of net and gross ecosystem carbon fluxes: A review *Agricultural and Forest Meteorology* **249** 520–33 Online: https://linkinghub.elsevier.com/retrieve/pii/S0168192317301806

Barbosa J M and Asner G P 2017 Effects of long-term rainfall decline on the structure and functioning of Hawaiian forests *Environmental Research Letters* **12** 094002 Online: https://doi.org/10.1088%2F1748-9326%2Faa7ee4

Birami B, Nägele T, Gattmann M, Preisler Y, Gast A, Arneth A and Ruehr N K 2020 Hot drought reduces the effects of elevated CO2 on tree water-use efficiency and carbon metabolism *New Phytologist* **226** 1607–21 Online: https://nph.onlinelibrary.wiley.com/doi/abs/10.1111/nph.16471

Bothwell L D, Selmants P C, Giardina C P and Litton C M 2014 Leaf litter decomposition rates increase with rising mean annual temperature in Hawaiian tropical montane wet forests *PeerJ* **2** e685 Online: https://peerj.com/articles/685

Cameron D R, Marvin D C, Remucal J M and Passero M C 2017 Ecosystem management and land conservation can substantially contribute to California's climate mitigation goals *Proceedings of the National Academy of Sciences* **114** 12833–8 Online: http://www.pnas.org/content/114/48/12833

Chapin F S, Woodwell G M, Randerson J T, Rastetter E B, Lovett G M, Baldocchi D D, Clark D A, Harmon M E, Schimel D S, Valentini R, Wirth C, Aber J D, Cole J J, Goulden M L, Harden J W, Heimann M, Howarth R W, Matson P A, McGuire A D, Melillo J M, Mooney H A, Neff J C, Houghton R A, Pace M L, Ryan M G, Running S W, Sala O E, Schlesinger W H and Schulze E-D 2006 Reconciling carbon-cycle concepts, terminology, and methods *Ecosystems* **9** 1041–50

Cuddihy L W and Stone C P 1990 *Alteration of Hawaiian vegetation: Effects of humans, their activities and introductions* (Honolulu, Hawaii: University of Hawaii Press)

Daniel C J, Frid L, Sleeter B M and Fortin M-J 2016 State-and-transition simulation models: A framework for forecasting landscape change *Methods in Ecology and Evolution* **7** 1413–23

Daniel C J, Sleeter B M, Frid L and Fortin M-J 2018 Integrating continuous stocks and flows into state-and-transition simulation models of landscape change *Methods in Ecology and Evolution* **9** 1133–43

Daniel C, Hughes J, Embrey A, Frid L and Lucet V 2020 *Rsyncrosim: The r interface to SyncroSim* Online: https://github.com/rsyncrosim/rsyncrosim

Del Grosso S, Parton W, Stohlgren T, Zheng D, Bachelet D, Prince S, Hibbard K and Olson R 2008 Global potential net primary production predicted from vegetation class, precipitation, and temperature *Ecology* **89** 2117–26

Don A, Schumacher J and Freibauer A 2011 Impact of tropical land-use change on soil organic carbon stocks – a meta-analysis *Global Change Biology* **17** 1658–70

Elison Timm O 2017 Future warming rates over the Hawaiian Islands based on elevation-dependent scaling factors *International Journal of Climatology* **37** 1093–104 Online: https://rmets.onlinelibrary.wiley.com/doi/abs/10.1002/joc.5065

Elison Timm O, Giambelluca T W and Diaz H F 2015 Statistical downscaling of rainfall changes in Hawai‘i based on the CMIP5 global model projections *Journal of Geophysical Research: Atmospheres* **120** 92–112

Fargione J E, Bassett S, Boucher T, Bridgham S D, Conant R T, Cook-Patton S C, Ellis P W, Falcucci A, Fourqurean J W, Gopalakrishna T, Gu H, Henderson B, Hurteau M D, Kroeger K D, Kroeger T, Lark T J, Leavitt S M, Lomax G, McDonald R I, Megonigal J P, Miteva D A, Richardson C J, Sanderman J, Shoch D, Spawn S A, Veldman J W, Williams C A, Woodbury P B, Zganjar C, Baranski M, Elias P, Houghton R A, Landis E, McGlynn E, Schlesinger W H, Siikamaki J V, Sutton-Grier A E and Griscom B W 2018 Natural climate solutions for the United States *Science Advances* **4** eaat1869 Online: https://advances.sciencemag.org/content/4/11/eaat1869

Foley J A, Prentice I C, Ramankutty N, Levis S, Pollard D, Sitch S and Haxeltine A 1996 An integrated biosphere model of land surface processes, terrestrial carbon balance, and vegetation dynamics *Global Biogeochemical Cycles* **10** 603–28

Fortini L B, Kaiser L R, Keith L M, Price J, Hughes R F, Jacobi J D and Friday J B 2019 The evolving threat of Rapid ‘ōhi‘a Death (ROD) to Hawai‘i’s native ecosystems and rare plant species *Forest Ecology and Management* **448** 376–85 Online: http://www.sciencedirect.com/science/article/pii/S0378112719301744

Franks P J, Adams M A, Amthor J S, Barbour M M, Berry J A, Ellsworth D S, Farquhar G D, Ghannoum O, Lloyd J, McDowell N, Norby R J, Tissue D T and Caemmerer S von 2013 Sensitivity of plants to changing atmospheric CO_2 concentration: From the geological past to the next century *New Phytologist* **197** 1077–94 Online: http://doi.wiley.com/10.1111/nph.12104

Frazier A G and Giambelluca T W 2017 Spatial trend analysis of Hawaiian rainfall from 1920 to 2012 *International Journal of Climatology* **37** 2522–31 Online: https://rmets.onlinelibrary.wiley.com/doi/abs/10.1002/joc.4862

Friedlingstein P, Jones M W, O’Sullivan M, Andrew R M, Hauck J, Peters G P, Peters W, Pongratz J, Sitch S, Quéré C L, Bakker D C E, Canadell J G, Ciais P, Jackson R B, Anthoni P, Barbero L, Bastos A, Bastrikov V, Becker M, Bopp L, Buitenhuis E, Chandra N, Chevallier F, Chini L P, Currie K I, Feely R A, Gehlen M, Gilfillan D, Gkritzalis T, Goll D S, Gruber N, Gutekunst S, Harris I, Haverd V, Houghton R A, Hurtt G, Ilyina T, Jain A K, Joetzjer E, Kaplan J O, Kato E, Klein Goldewijk K, Korsbakken J I, Landschützer P, Lauvset S K, Lefèvre N, Lenton A, Lienert S, Lombardozzi D, Marland G, McGuire P C, Melton J R, Metzl N, Munro D R, Nabel J E M S, Nakaoka S-I, Neill C, Omar A M, Ono T, Peregon A, Pierrot D, Poulter B, Rehder G, Resplandy L, Robertson E, Rödenbeck C, Séférian R, Schwinger J, Smith N, Tans P P, Tian H, Tilbrook B, Tubiello F N, Werf G R van der, Wiltshire A J and Zaehle S 2019 Global Carbon Budget 2019 *Earth System Science Data* **11** 1783–838 Online:

https://essd.copernicus.org/articles/11/1783/2019/

Galarraga I, Murieta E S de and França J 2017 Climate policy at the sub-national level *Trends in Climate Change Legislation* ed A Averchenkova, S Fankhauser and M Nachmany (Edward Elgar Publishing) pp 143–74 Online: https://www.elgaronline.com/view/9781786435774.00018.xml

Giambelluca T W, Chen Q, Frazier A G, Price J P, Chen Y-L, Chu P-S, Eischeid J K and Delparte D M 2013 Online Rainfall Atlas of Hawaiʻi *Bull. Amer. Meteor. Soc.* **94** 313–6

Giambelluca T W, Diaz H F and Luke M S A 2008 Secular temperature changes in Hawaiʻi *Geophysical Research Letters* **35** Online: https://agupubs.onlinelibrary.wiley.com/doi/abs/10.1029/2008GL034377

Giambelluca T W, Shuai X, Barnes M L, Alliss R J, Longman R J, Miura T, Chen Q, Frazier A G, Mudd R G, Cuo L and Businger A D 2014 *Evapotranspiration of Hawaiʻi* Online: http://evapotranspiration.geography.hawaii.edu/downloads.html

Griscom B W, Adams J, Ellis P W, Houghton R A, Lomax G, Miteva D A, Schlesinger W H, Shoch D, Siikamäki J V, Smith P, Woodbury P, Zganjar C, Blackman A, Campari J, Conant R T, Delgado C, Elias P, Gopalakrishna T, Hamsik M R, Herrero M, Kiesecker J, Landis E, Laestadius L, Leavitt S M, Minnemeyer S, Polasky S, Potapov P, Putz F E, Sanderman J, Silvius M, Wollenberg E and Fargione J 2017 Natural climate solutions *Proceedings of the National Academy of Sciences* **114** 11645–50 Online: https://www.pnas.org/content/114/44/11645

He L, Chen J M, Croft H, Gonsamo A, Luo X, Liu J, Zheng T, Liu R and Liu Y 2017 Nitrogen Availability Dampens the Positive Impacts of CO2 Fertilization on Terrestrial Ecosystem Carbon and Water Cycles *Geophysical Research Letters* **44** 11, 590–11, 600 Online: https://agupubs.onlinelibrary.wiley.com/doi/abs/10.1002/2017GL075981

Hijmans R J 2020 *Raster: Geographic data analysis and modeling* Online: https://CRAN.R-project.org/package=raster

Jackson R B, Lajtha K, Crow S E, Hugelius G, Kramer M G and Piñeiro G 2017 The Ecology of Soil Carbon: Pools, Vulnerabilities, and Biotic and Abiotic Controls *Annual Review of Ecology, Evolution, and Systematics* **48** 419–45 Online: http://www.annualreviews.org/doi/10.1146/annurev-ecolsys-112414-054234

Jacobi J D, Price J P, Gon III S M and Berkowitz P 2017 Hawaii Land Cover and Habitat Status: U.s. Geological Survey data release Online: https://doi.org/10.5066/F7DB80B9

Jiang M, Medlyn B E, Drake J E, Duursma R A, Anderson I C, Barton C V M, Boer M M, Carrillo Y, Castañeda-Gómez L, Collins L, Crous K Y, De Kauwe M G, Santos B M dos, Emmerson K M, Facey S L, Gherlenda A N, Gimeno T E, Hasegawa S, Johnson S N, Kännaste A, Macdonald C A, Mahmud K, Moore B D, Nazaries L, Neilson E H J, Nielsen U N, Niinemets Ü, Noh N J, Ochoa-Hueso R, Pathare V S, Pendall E, Pihlblad J, Piñeiro J, Powell J R, Power S A, Reich P B, Renchon A A, Riegler M, Rinnan R, Rymer P D, Salomón R L, Singh B K, Smith B, Tjoelker M G, Walker J K M, Wujeska-Klause A, Yang J, Zaehle S and Ellsworth D S 2020 The fate of carbon in a mature forest under carbon dioxide enrichment *Nature* **580** 227–31 Online: https://www.nature.com/articles/s41586-020-2128-9

Keenan T F and Williams C A 2018 The Terrestrial Carbon Sink *Annual Review of Environment and Resources* **43** 219–43 Online: https://doi.org/10.1146/annurev-environ-102017-030204

Kim Y-S and Bai J 2018 *Population and economic projections for the State of Hawaii to 2045* (Hawaii Department of Business, Economic Development & Tourism) Online: https://dbedt.hawaii.gov/economic/economic-forecast/2045-long-range-forecast/

Kimball H L, Selmants P C, Moreno A, Running S W and Giardina C P 2017 Evaluating the role of land cover and climate uncertainties in computing gross primary production in Hawaiian Island ecosystems *PLOS ONE* **12** e0184466 Online: http://journals.plos.org/plosone/article?id=10.1371/journal.pone.0184466

Kurz W A, Dymond C C, White T M, Stinson G, Shaw C H, Rampley G J, Smyth C, Simpson B N, Neilson E T, Trofymow J A, Metsaranta J and Apps M J 2009 CBM-CFS3: A model of carbon-dynamics in forestry and land-use change implementing IPCC standards *Ecological Modelling* **220** 480–504 Online: http://www.sciencedirect.com/science/article/pii/S0304380008005012

Kuzyakov Y and Gavrichkova O 2010 Time lag between photosynthesis and carbon dioxide efflux from soil: A review of mechanisms and controls *Global Change Biology* **16** 3386–406 Online: http://doi.wiley.com/10.1111/j.1365-2486.2010.02179.x

Liu J, Sleeter B M, Zhu Z, Loveland T R, Sohl T, Howard S M, Key C H, Hawbaker T, Liu S, Reed B, Cochrane M A, Heath L S, Jiang H, Price D T, Chen J M, Zhou D, Bliss N B, Wilson T, Sherba J, Zhu Q, Luo Y and Poulter B 2020 Critical land change information enhances the understanding of carbon balance in the United States *Global Change Biology* **26** 3920–9 Online: https://onlinelibrary.wiley.com/doi/abs/10.1111/gcb.15079

McKenzie M M, Giambelluca T W and Diaz H F 2019 Temperature trends in Hawaiʻi: A century of change, 1917–2016 *International Journal of Climatology* **39** 3987–4001 Online: https://rmets.onlinelibrary.wiley.com/doi/abs/10.1002/joc.6053

Mokany K, Raison R J and Prokushkin A S 2006 Critical analysis of root : Shoot ratios in terrestrial biomes *Global Change Biology* **12** 84–96 Online: http://doi.wiley.com/10.1111/j.1365-2486.2005.001043.x

Mortenson L A, Flint Hughes R, Friday J B, Keith L M, Barbosa J M, Friday N J, Liu Z and Sowards T G 2016 Assessing spatial distribution, stand impacts and rate of Ceratocystis fimbriata induced ʻōhiʻa (Metrosideros polymorpha) mortality in a tropical wet forest, Hawaiʻi Island, USA *Forest Ecology and Management* **377** 83–92 Online: https://www.sciencedirect.com/science/article/pii/S0378112716303231

NOAA 2020 *Coastal Change Analysis Program (C-CAP) Regional Land Cover: Hawaii* (NOAA Office of Coastal Management) Online: https://coast.noaa.gov/digitalcoast/data/

Norby R J, DeLucia E H, Gielen B, Calfapietra C, Giardina C P, King J S, Ledford J, McCarthy H R, Moore D J P, Ceulemans R, Angelis P D, Finzi A C, Karnosky D F, Kubiske M E, Lukac M, Pregitzer K S, Scarascia-Mugnozza G E, Schlesinger W H and Oren R 2005 Forest response to elevated CO2 is conserved across a broad range of productivity *Proceedings of the National Academy of Sciences* **102** 18052–6 Online: https://www.pnas.org/content/102/50/18052

Norby R J, Warren J M, Iversen C M, Medlyn B E and McMurtrie R E 2010 CO2 enhancement of forest productivity constrained by limited nitrogen availability *Proceedings of the National Academy of Sciences* **107** 19368–73 Online: https://www.pnas.org/content/107/45/19368

Obermeier W A, Lehnert L W, Kammann C I, Müller C, Grünhage L, Luterbacher J, Erbs M, Moser G, Seibert R, Yuan N and Bendix J 2017 Reduced CO 2 fertilization effect in temperate C3 grasslands under more extreme weather conditions *Nature Climate Change* **7** 137–41 Online: https://www.nature.com/articles/nclimate3191

Osher L J, Matson P A and Amundson R 2003 Effect of land use change on soil carbon in Hawaii *Biogeochemistry* **65** 213–32 Online: https://doi.org/10.1023/A:1026048612540

Perroy R L, Melrose J and Cares S 2016 The evolving agricultural landscape of post-plantation Hawaiʻi *Applied Geography* **76** 154–62 Online: http://linkinghub.elsevier.com/retrieve/pii/S0143622816304490

Prestele R, Arneth A, Bondeau A, Noblet-Ducoudré N de, Pugh T A M, Sitch S, Stehfest E and Verburg P H 2017 Current challenges of implementing anthropogenic land-use and land-cover change in models contributing to climate change assessments *Earth System Dynamics* **8** 369–86 Online: https://esd.copernicus.org/articles/8/369/2017/

R Core Team 2019 *R: A language and environment for statistical computing* (Vienna, Austria: R Foundation for Statistical Computing) Online: https://www.R-project.org/

Reich P B, Hobbie S E, Lee T, Ellsworth D S, West J B, Tilman D, Knops J M H, Naeem S and Trost J 2006 Nitrogen limitation constrains sustainability of ecosystem response to CO2 *Nature* **440** 922–5 Online: http://www.nature.com/articles/nature04486

Schuur E A 2003 Productivity and global climate revisited: The sensitivity of tropical forest growth to precipitation *Ecology* **84** 1165–70

Selmants P C, Giardina C P, Jacobi J D and Zhu Z 2017 *Baseline and projected future carbon storage and carbon fluxes in ecosystems of Hawai'i* (U.S. Geological Survey) Online: https://doi.org/10.3133/pp1834

Sleeter B M, Liu J, Daniel C, Rayfield B, Sherba J, Hawbaker T J, Zhiliang Zhu, Selmants P C and Loveland T R 2018 Effects of contemporary land-use and land-cover change on the carbon balance of terrestrial ecosystems in the United States *Environ. Res. Lett.* **13** 045006 Online: http://stacks.iop.org/1748-9326/13/i=4/a=045006

Sleeter B M, Marvin D C, Cameron D R, Selmants P C, Westerling A L, Kreitler J, Daniel C J, Liu J and Wilson T S 2019 Effects of 21st-century climate, land use, and disturbances on ecosystem carbon balance in California *Global Change Biology* **25** 3334–53

Sleeter B M, Wilson T S, Sharygin E and Sherba J T 2017 Future scenarios of land change based on empirical data and demographic trends *Earth's Future* **5** 1068–83 Online: http://doi.wiley.com/10.1002/2017EF000560

Soil Survey Staff 2016 *Soil Survey Geographic (SSURGO) Database, Natural Resources Conservation Service, United States Department of Agriculture* (Natural Resources Conservation Service, USDA) Online: https://sdmdataaccess.sc.egov.usda.gov.

State of Hawai'i 2019 *Hawaii Greenhouse Gas Emissions Report for 2015* (Hawaii State Department of Health, Clean Air Branch) Online: https://health.hawaii.gov/cab/files/2019/02/2015-Inventory_Final-Report_January-2019-004-1.pdf

Sun Q, Miao C, Hanel M, Borthwick A G L, Duan Q, Ji D and Li H 2019 Global heat stress on health, wildfires, and agricultural crops under different levels of climate warming *Environment International* **128** 125–36 Online: http://www.sciencedirect.com/science/article/pii/S0160412018328654

Suryanata K 2009 Diversified Agriculture, Land Use, and Agrofood Networks in Hawaii

Economic Geography **78** 71–86 Online: http://doi.wiley.com/10.1111/j.1944-8287.2002.tb00176.x

Terrer C, Jackson R B, Prentice I C, Keenan T F, Kaiser C, Vicca S, Fisher J B, Reich P B, Stocker B D, Hungate B A, Peñuelas J, McCallum I, Soudzilovskaia N A, Cernusak L A, Talhelm A F, Sundert K V, Piao S, Newton P C D, Hovenden M J, Blumenthal D M, Liu Y Y, Müller C, Winter K, Field C B, Viechtbauer W, Lissa C J V, Hoosbeek M R, Watanabe M, Koike T, Leshyk V O, Polley H W and Franklin O 2019 Nitrogen and phosphorus constrain the CO2 fertilization of global plant biomass *Nature Climate Change* 1–6 Online: https://www.nature.com/articles/s41558-019-0545-2

Trauernicht C 2019 Vegetation—Rainfall interactions reveal how climate variability and climate change alter spatial patterns of wildland fire probability on Big Island, Hawaii *Science of The Total Environment* **650** 459–69 Online: http://www.sciencedirect.com/science/article/pii/S0048969718333187

Trauernicht C, Pickett E, Giardina C P, Litton C M, Cordell S and Beavers A 2015 The contemporary scale and context of wildfire in Hawai'i *Pacific Science* **69** 427–44

Vaughn N R, Asner G P, Brodrick P G, Martin R E, Heckler J W, Knapp D E and Hughes R F 2018 An Approach for High-Resolution Mapping of Hawaiian Metrosideros Forest Mortality Using Laser-Guided Imaging Spectroscopy *Remote Sensing* **10** 502 Online: https://www.mdpi.com/2072-4292/10/4/502

Walker A P, De Kauwe M G, Medlyn B E, Zaehle S, Iversen C M, Asao S, Guenet B, Harper A, Hickler T, Hungate B A, Jain A K, Luo Y, Lu X, Lu M, Luus K, Megonigal J P, Oren R, Ryan E, Shu S, Talhelm A, Wang Y-P, Warren J M, Werner C, Xia J, Yang B, Zak D R and Norby R J 2019 Decadal biomass increment in early secondary succession woody ecosystems is increased by CO2 enrichment *Nature Communications* **10** Online: http://www.nature.com/articles/s41467-019-08348-1

Walker A P, Kauwe M G D, Bastos A, Belmecheri S, Georgiou K, Keeling R, McMahon S M, Medlyn B E, Moore D J P, Norby R J, Zaehle S, Anderson-Teixeira K J, Battipaglia G, Brienen R J W, Cabugao K G, Cailleret M, Campbell E, Canadell J, Ciais P, Craig M E, Ellsworth D, Farquhar G, Fatichi S, Fisher J B, Frank D, Graven H, Gu L, Haverd V, Heilman K, Heimann M, Hungate B A, Iversen C M, Joos F, Jiang M, Keenan T F, Knauer J, Körner C, Leshyk V O, Leuzinger S, Liu Y, MacBean N, Malhi Y, McVicar T, Penuelas J, Pongratz J, Powell A S, Riutta T, Sabot M E B, Schleucher J, Sitch S, Smith W K, Sulman B, Taylor B, Terrer C, Torn M S, Treseder K, Trugman A T, Trumbore S E, Mantgem P J van, Voelker S L, Whelan M E and Zuidema P A 2020 Integrating the evidence for a terrestrial carbon sink caused by increasing atmospheric CO2 *New Phytologist* **229** 2413–45

Wickham H, Averick M, Bryan J, Chang W, McGowan L D, François R, Grolemund G, Hayes A, Henry L, Hester J, Kuhn M, Pedersen T L, Miller E, Bache S M, Müller K, Ooms J, Robinson D, Seidel D P, Spinu V, Takahashi K, Vaughan D, Wilke C, Woo K and Yutani H 2019 Welcome to the tidyverse *Journal of Open Source Software* **4** 1686

Yang J, Medlyn B E, Kauwe M G D, Duursma R A, Jiang M, Kumarathunge D, Crous K Y, Gimeno T E, Wujeska-Klause A and Ellsworth D S 2020 Low sensitivity of gross primary production to elevated CO2 in a mature eucalypt woodland *Biogeosciences* **17** 265–79 Online: https://www.biogeosciences.net/17/265/2020/

Zhu Z, Piao S, Myneni R B, Huang M, Zeng Z, Canadell J G, Ciais P, Sitch S, Friedlingstein P, Arneth A, Cao C, Cheng L, Kato E, Koven C, Li Y, Lian X, Liu Y, Liu R, Mao J, Pan Y, Peng S, Peñuelas J, Poulter B, Pugh T A M, Stocker B D, Viovy N, Wang X, Wang Y, Xiao Z, Yang H, Zaehle S and Zeng N 2016 Greening of the Earth and its drivers *Nature Climate Change* **6** 791–5 Online: https://www.nature.com/articles/nclimate3004

Ziegler A C 2002 *Hawaiian Natural History, Ecology, and Evolution* (Honolulu, Hawaii: University of Hawaii Press)